

Absolute dimensions of eclipsing binaries

XXI. V906 Scorpii: a triple system member of M 7*

S.H.P. Alencar¹, L.P.R. Vaz¹, and B.E. Helt²

¹ Departamento de Física, ICEx, UFMG, Caixa Postal 702, 30.161-970 Belo Horizonte, MG, Brazil

² Niels Bohr Institute for Astronomy, Physics and Geophysics; Astronomical Observatory, Juliane Maries Vej 30, DK-2100 Copenhagen, Denmark

Received 24 December 1996 / Accepted 29 April 1997

Abstract. We present an analysis based on new *wvby* light curves and spectroscopic data of the detached triple-lined B-type eclipsing binary V906 Sco. The *wvby* light curves are analysed with an extended version of the Wilson-Devinney program. The spectroscopic CCD observations are analysed with both the Sterne and the Lehmann-Filhés methods. We conclude from the combined analysis that the triple system V906 Sco is a member of the open cluster M 7 and that its B-type eclipsing components are still on the main sequence, at an age of $(2.4 \pm 0.3) \times 10^8$ yrs, already close to the TAMS (especially the more massive one). The system is older than the time for circularization of the orbit, and the small eccentricity is probably caused by the third component, which, however, is unlikely to be the main responsible for the apsidal motion, probably more influenced by tidal and rotational deformation. We determine absolute dimensions of high precision (errors $< 2\%$): $M_A = 3.25 \pm 0.07$, $R_A = 3.52 \pm 0.04$, $M_B = 3.38 \pm 0.07$ and $R_B = 4.52 \pm 0.04$, in solar units. The system is detached, with both components in synchronous rotation, and therefore representative for normal stars.

Key words: binaries: eclipsing – stars: fundamental parameters – stars: evolution – stars: individual: V906 Sco

1. Introduction

The variability of V906 Sco was discovered by Koelbloed (1959) in a photometric study of M 7. Feinstein (1961) observed spectroscopically several stars in the cluster and noticed the variable radial velocity of the system. Abt et al. (1970) obtained orbital elements for the system from 6 spectra at 62 Å/mm

Send offprint requests to: L.P.R. Vaz

* Based on observations collected with the 1.6 m telescope of the Pico dos Dias Observatory, National Laboratory of Astrophysics, LNA-CNPq, Brasópolis, MG, Brazil and with the Danish 50 cm telescope (SAT) at the European Southern Observatory (ESO), La Silla, Chile

Table 1. Data for V906 Sco and the comparison stars.

	V906 Sco	Comp. 1	Comp. 2	Comp. 3
HD	162724	162631	162817	161390
SAO	209428	209422	209446	209246
α_{1950}	17 ^h 50 ^m 35 ^s	17 ^h 50 ^m 15 ^s	17 ^h 51 ^m 08 ^s	17 ^h 43 ^m 41 ^s
δ_{1950}	−34° 44′ 35″	−34° 51′ 20″	−34° 27′ 28″	−38° 05′ 37″
Sp. type	B9 V	A0	A0	B9
V (0 ^p 25)	5.96 ±1	7.40 ±1	6.12 ±1	6.43 ±1
$b - y$	0.032 ±3	0.044 ±3	0.063 ±2	−0.002 ±1
m_1	0.100 ±3	0.126 ±4	0.094 ±2	136 ±2
c_1	0.972 ±3	1.023 ±5	1.183 ±2	0.878 ±7
β (0 ^p 239)	2.801 ±3	2.861 ±4	2.811 ±3	2.843 ±4

dispersion and 4 at 39 Å/mm, but the velocities were poorly determined, having mean errors of 57 km/s per spectrum. Due to the large scatter in the velocity curve, the orbit was found to be far more eccentric ($e = 0.18 \pm 0.12$) than it really is. Leung & Schneider (1975) published light curves (UBV) of V906 Sco and obtained a photometric solution with the Wilson-Devinney model in its original (1971) version. They assumed a circular orbit and found the system to be detached.

In all the papers quoted V906 Sco was analysed as a double system in spite of the fact that van den Bos (1931) had found it to be a visual binary and that the Index Catalogue of Visual Double Stars includes it as B 1871 quoting that the separation has decreased from 0′.3 to 0′.1 between 1929 and 1957. Eggen (1981) noted that V906 Sco has a close companion although his reference is incorrect. No visual components could be separated during our observations. Lacy & Evans (1979) communicated that the system was triple-lined in high resolution scans. No further photometric or spectroscopic analysis has been published since then, motivating this new analysis with due allowance for third light and the triple lined spectra.

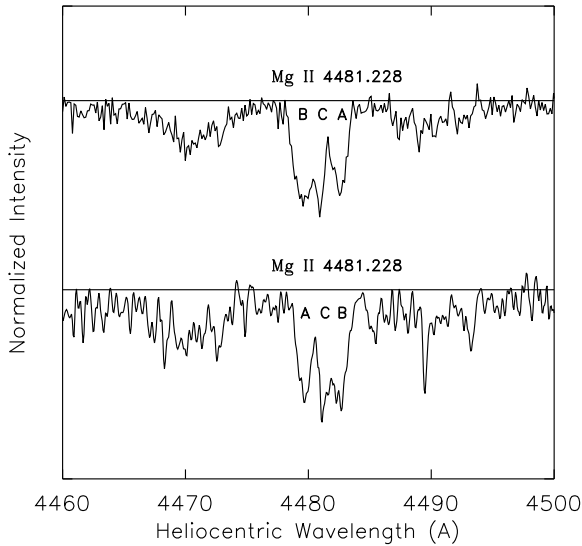


Fig. 1. Spectra of V906 Sco at phases $\phi = 0.88$ (top) and $\phi = 0.39$ (bottom) for Mg II 4481.228 Å. The continuum level is shown for each spectrum.

Table 2. Lines measured in V906 Sco

Wavelength (Å)	lines
4481.228	Mg II
4549.467	Fe II, Ti II
5018.434	Fe II
5041.063	Si II
5056.020	Si II

Since the system is a possible member of the open cluster NGC 6475 (Messier 7, Snowden 1976; Eggen 1981), the determination of its physical parameters will allow us to compare the cluster age and distance, determined as usual for clusters, with the independently determined age and distance for V906 Sco.

We have obtained complete high precision *wavy* light curves, additional H_{β} photometry and high precision spectroscopic observations of V906 Sco. We present here the analysis of these data, the detailed photometric data being published separately (Vaz et al. 1997). Our results show that V906 Sco is a detached system, well suited for precise determination of masses and radii of its components, which are evolved main sequence stars that provide a good test of single-star evolution models. The orbit was found to be slightly eccentric and our analysis suggests apsidal motion. General information concerning the system and the comparison stars is given in Table 1.

2. Spectroscopic analysis

V906 Sco was observed between 1989 and 1995 with the 1.6 m telescope and coude spectrograph at Pico dos Dias Observatory (PDO), National Laboratory for Astrophysics (LNA-CNPq) at Brasópolis-MG, Brazil. In 1989 and 1990 an EEV CCD (386×576 22 μm square pixels) P8603S chip was used with a

model #1 (serial no. 48) camera and acquisition program (AT1, version 3.1) from Wright Instruments Ltd. at a mean dispersion of 18.1 Å/mm (0.397 Å/pix, corresponding to ~ 230 Å covered in each frame), with a projected slit width of 1.40 pixel. The average exposure time was ~ 5 min in the frames centered at 5000 Å. The grating (Milton Roy Co.) used during this period has 600 lines/mm blazed for 8000 Å ($13^{\circ}53'$ blaze angle). From 1992 to 1995 the observations were performed with an EEV CCD05-20-0-202 (770×1152 22.5 μm square pixels, grade 0) chip with UV coating at a mean dispersion of 5.84 Å/mm (0.131 Å/pix, ~ 150 Å covered per frame), with a projected slit of 1.37 pixel. We used an 1800 lines/mm holographic grating (Jobin Yvon) blazed from 3000 Å to 7500 Å and the spectra were exposed for 20 min.

The spectra show triple lines of different widths and depths (Fig. 1). Star A, the hotter component eclipsed in the primary minimum, has slightly narrower and weaker lines than component B, while component C has very narrow lines easily distinguishable from the other ones.

2.1. Radial-velocity curves and the mass ratio

We reduced all spectra with a C program (Vieira 1991, 1993) using the optimum extraction algorithm by Horne (1986). After wavelength calibration and normalization of the spectra, the radial velocities were measured by simultaneously fitting (least-squares) triple gaussian or lorentzian curves to the lines listed in Table 2, taking account, in this way, of possible line blending. The small number of lines available impeded the use of cross-correlation functions (e.g. Hill & Khamseh 1991), but our method has already been successfully tested (Vaz et al. 1995) and does not introduce systematic effects. The radial velocities obtained are shown in Table 3 (columns 3, 7 and 11) and in Fig. 2. Small corrections to the measured values were made in order to take into account the proximity effect of the components. These corrections were taken from the final solutions determined with the Wilson-Devinney code (Sect. 3.3.2).

The spectroscopic solutions were made with the program SBOP (Etzel 1985) which allows the use of the methods of Wilsing-Russell (Wolfe Jr. et al. 1967), Sterne (1941) or Lehmann-Filhés (1894). The latter allows solving simultaneously for the orbital elements of both components (solutions L-F in Table 4), while Sterne's method is more adequate for small orbital eccentricities, although it must be applied to each component separately.

The solutions in Table 4 were obtained with the photometric ephemeris derived in Sect. 3.2. In solution L-F 1, where all parameters were adjusted (excepting the period), the derived orbital elements have small errors except for e , the orbital eccentricity and ω , the angle of periastron passage, which were not accurately determined. Although a circular orbit also fits the spectroscopic data, we can not assume it because the photometric data show clearly that the orbit is eccentric (Sect. 3.1): the difference in phase between the secondary and the primary minima in the light curves is 0.5031 ± 0.0004 . The indeterminacy of e and ω is not removed in solutions Sterne 1/2, applied to the

Table 3. Radial velocity observations of V906 Sco (km/s)

HJD - 2440000	phase	star w A	O-C	WD corr.	star w B	O-C	WD corr.	star C		
7666.6809	0.6081	82.3	1	10.0	-0.1	-103.1	1	-4.2	-0.2	-18.9
7666.7811	0.6441	102.1	1	7.3	-0.1	-124.6	1	-3.9	-0.1	-3.2
7666.7881	0.6466	104.3	1	8.1	-0.1	-120.6	1	1.5	-0.1	-14.1
7666.8423	0.6661	100.2	1	-5.8	-0.1	-138.6	1	-7.1	-0.0	-7.4
7666.8492	0.6686	115.8	1	8.7	-0.1	-139.9	1	-7.4	-0.0	-10.1
7668.6334	0.3090	-131.6	.5	13.8	0.1	106.3	1	-4.2	-0.1	-21.0
7728.6747	0.8605	72.2	0	-21.8	-0.1	-128.1	1	-8.3	0.2	-7.8
7754.4783	0.1225	-109.5	1	3.4	0.0	80.3	1	1.1	-0.2	-2.8
7756.6628	0.9066	63.0	1	-0.5	-0.0	-91.5	1	-0.9	0.1	-13.8
8021.8423	0.0913	-107.5	.5	-16.1	0.0	49.1	1	-9.4	-0.1	-9.2
8079.6611	0.8451	91.8	1	-10.4	-0.1	-123.3	1	4.4	0.2	-5.2
8080.5919	0.1792	-134.4	1	7.3	0.1	110.7	1	3.9	-0.2	-19.1
8080.6233	0.1904	-150.9	1	-5.4	0.1	100.4	1	-10.1	-0.3	-14.3
8813.6830	0.3181	-140.1	1	2.2	0.1	105.6	1	-1.9	-0.0	-12.2
8813.7080	0.3271	-137.5	1	1.5	0.1	107.1	1	2.8	-0.0	-10.4
8816.5660	0.3529	-121.5	1	5.4	0.1	92.7	1	0.0	0.0	-11.6
8816.5701	0.3544	-124.0	1	2.2	0.1	95.7	1	3.8	0.1	-11.7
8816.5759	0.3565	-123.5	1	1.5	0.1	96.3	1	5.5	0.1	-11.6
8816.5919	0.3622	-120.9	1	1.0	0.1	82.8	1	-5.0	0.1	-13.6
8816.6112	0.3691	-119.6	1	-1.7	0.1	84.4	1	0.4	0.1	-9.3
8816.6698	0.3902	-103.3	1	1.3	0.1	83.9	.5	12.7	0.2	-3.2
8816.6817	0.3944	-94.4	1	7.3	0.1	67.9	1	-0.4	0.2	-3.7
8816.6965	0.3997	-94.7	1	3.3	0.1	64.4	1	-0.3	0.2	-3.7
8816.7166	0.4070	-95.8	1	-3.0	0.0	66.5	1	6.7	0.2	-9.0
8816.7678	0.4254	-89.2	1	-10.2	0.0	57.8	1	11.2	0.2	-9.0
8849.4659	0.1622	-133.2	1	1.4	0.1	98.9	1	-1.1	-0.2	-14.4
8849.4942	0.1723	-142.3	1	-3.4	0.1	98.0	1	-6.2	-0.2	-16.2
8849.5133	0.1792	-139.7	1	2.0	0.1	106.0	1	-0.8	-0.2	-6.4
8849.5535	0.1936	-144.2	1	2.3	0.1	109.9	1	-1.5	-0.3	-12.4
8849.5733	0.2007	-149.2	1	-0.7	0.1	110.0	1	-3.4	-0.3	-14.3
8851.4543	0.8759	75.2	1	-9.6	-0.0	-109.0	1	2.0	0.2	-16.8
8851.4705	0.8817	86.9	1	5.9	-0.0	-100.8	1	6.6	0.2	-9.3
8851.6145	0.9334	49.2	1	6.2	0.7	-81.7	1	-11.3	0.0	-14.7
8852.4747	0.2421	-156.1	1	-1.3	0.1	116.2	1	-3.3	-0.2	-13.5
8852.5225	0.2593	-154.5	1	0.2	0.1	113.4	1	-6.0	-0.2	-14.9
9823.7673	0.8822	86.8	1	6.1	-0.0	-108.1	1	-1.1	0.1	-15.6

individual components separately. However, the agreement between the system velocity from these individual solutions makes us confident that we reduced efficiently (if not removed) the possible blending among the lines of stars B and C. In Sect. 3.3.1 this problem is discussed in detail and acceptable ranges of values are established ($0.0048 \leq e \leq 0.0074$, $-20^\circ < \omega < 50^\circ$). The adopted spectroscopic solution is shown in the second column of Table 4 and as solid lines in Fig. 2. It was calculated with the adopted final photometric solution ($\omega = 40^\circ$, Sect. 3.3.2), and is in complete agreement with both the spectroscopic and the photometric data.

At first sight, our adopted mass ratio disagrees with values published for V906 Sco by Abt et al. (1970), $q = 0.79 \pm 0.15$, and by Leung & Schneider (1975), $q = 0.885 \pm 0.012$. The former called the **more massive** star the primary, the opposite of what is done in the present work where the **primary** is the hotter and less massive component eclipsed during primary minimum. The ratio to be compared with ours is then the inverse of the value published by Abt et al. (1970), $q = 1.27 \pm 0.24$, in agreement with our value. Leung & Schneider used the same notation as we do. However, their mass ratio is obtained not from spectroscopy but from their photometric solution, with no allowance for third light.

Table 4. Spectroscopic orbital elements for V906 Sco. Numbers between parentheses were calculated from the converged parameters.

Element	L-F 1	L-F 2 (adopted)	Sterne 1 primary	Sterne 2 secondary
T_0 (-2440000)	11338 ^d 87 ± 15	8355 ^d 5170 ± 37	8405 ^d 3470 ± 54	8334 ^d 3183 ± 46
$e \cos \omega$	(0.021) (± 13)	(0.0041) (± 6)	0.008 ± 20	-0.019 ± 16
$e \sin \omega$	(-0.0041) (± 93)	(0.0035) (± 5)	-0.003 ± 0.010	0.011 ± 0.008
e	0.0217 ± 119	0.0054 ± 8	(0.0085) (± 189)	(0.0217) (± 146)
ω_{primary} ($^\circ$)	349 ± 19	40 (fixed)	(338) (± 113)	(*329) (± 14)
V_0 (km s^{-1})	-15.04 ± 0.74	-15.04 ± 0.76	-13.6 ± 1.8	-16.4 ± 1.5
K_A (km s^{-1})	140.9 ± 1.5	140.5 ± 1.3	141.6 ± 1.6	- -
K_B (km s^{-1})	135.8 ± 1.4	135.3 ± 1.3	- -	136.2 ± 1.3
$a_A \sin i$ (R_\odot)	7.77 ± 8	7.73 ± 7	7.79 ± 9	- -
$a_B \sin i$ (R_\odot)	7.49 ± 8	7.45 ± 7	- -	7.49 ± 7
$M_A \sin^3 i$ (M_\odot)	3.019 ± 55	2.969 ± 50	3.03 ± 15	- -
$M_B \sin^3 i$ (M_\odot)	3.132 ± 57	3.083 ± 51	- -	3.15 ± 17
M_B/M_A	1.038 ± 15	1.038 ± 14	- -	1.040 ± 21
$\sigma(1 \text{ obs.})$	5.5	5.7	6.1	5.0
$^* \omega_{\text{primary}} =$		$\omega_{\text{secondary}} +$	180°	

2.2. Rotation rates and luminosity ratios

The widths (FWHM) of the lines Mg II (4481.228 Å) and Fe II (5018.434 Å) in V906 Sco were interpolated between those of the selected standard stars for projected rotation velocity from Slettebak et al. (1975), given in Table 5. We found the following rotational velocities for V906 Sco: $v_A \sin i = 62 \pm 8 \text{ km s}^{-1}$, $v_B \sin i = 80 \pm 5 \text{ km s}^{-1}$ and $v_C \sin i = 8 \pm 4 \text{ km s}^{-1}$. The rotational velocity of component C is close to the limit of detection but we can safely assume that its value is smaller than 10 km s^{-1} .

It is possible to calculate the luminosity ratios between the three components by using the equivalent widths of lines for which the dependence of line strength on temperature is known. The third component of V906 Sco does rotate more slowly than the eclipsing pair but should have a spectral type close to that of the pair (B9). This can be inferred from the fact that its lines are very similar to the lines of the eclipsing pair in essentially all features measured. We can then use the Mg II (4481 Å, see Fig. 1) line which, according to Andersen et al. (1984, 1990a),

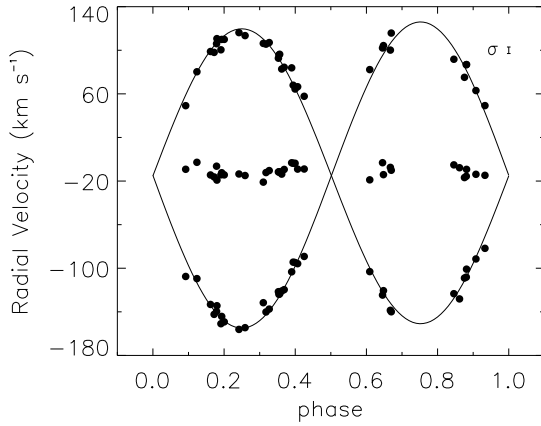


Fig. 2. Observed and theoretical radial velocity curves of V906 Sco. The bar at the upper right part of the figure is the mean error ($\sigma = 6 \text{ km s}^{-1}$) of one observation.

Table 5. Standard stars for rotational velocity.

Star	Sp. type	$V \sin i$ (km s^{-1})
HD 181454	B8 IV	75
HD 207971	B8 III	55
HD 16978	B9 IV	90
HD 196867	B9 IV	140
HD 181869	B9 III	70
HD 176437	B9 III	60
HD 146624	A0 V	30
HD 188228	A0 V	60

does not change significantly with temperature in this spectral range, where its line strength is close to maximum.

The observed normalized spectrum is a linear combination of the individual intrinsic spectra of each component. The FWHM of individual lines are not affected, but the intensity of each line is diluted in the continuum light of the other stars. Assuming that the line strength is equal for all three stars, which is in this case a good approximation, observed and intrinsic equivalent widths for each star (represented by the index i) are related by

$$[EW]_{\text{obs},i} = a_i [EW]_{\text{intr},i} \quad (i = A, B, C), \quad (1)$$

where a_i is the relative continuum level of component i , and $a_A + a_B + a_C = 1$. Our measurements of the observed equivalent width and FWHM yield for the eclipsing pair:

$$\frac{[EW]_{\text{obs}, B}}{[EW]_{\text{obs}, A}} = \frac{L_B}{L_A} = 1.35 \pm 0.12. \quad (2)$$

For the third component we used the observed equivalent widths and the FWHM measured for the three stars and determined its contribution in terms of the eclipsing ones (i.e. with the third light parameter in the same units as used in the light curve solutions, Sect. 3.3). We took into account that the FWHM of

the lines does not change in the combined spectrum compared to the intrinsic values:

$$\frac{L_C}{L_A + L_B} = L_3 = 0.196 \pm 0.014. \quad (3)$$

An error in the assumption of equal depths influences the result in such a way that 10% variation in the line strength of either component A or component B causes 10% variation in L_B/L_A and 5% in the relative contribution of the third component. On the other hand, the line strength of component C does not affect L_B/L_A , but 10% variation in it induces changes of $\sim 10\%$ in the L_3 parameter.

3. Photometric analysis

3.1. Observations

The photometric observations were made from 1987 to 1991 with the Strömgren Automatic Telescope (SAT) at ESO, La Silla, Chile, equipped with the six-channel spectrograph-photometer and photon counting system described by Nielsen et al. (1987), and using a circular diaphragm of $13''$ diameter. HD 162631, HD 162817, and HD 161390 were used as comparison stars and no variation was noted among them during the observing period. The mean errors of a magnitude difference between the comparison stars are 0^m005 (colour u) and 0^m004 (vby).

The light curves of V906 Sco, with 1117 magnitude differences in each colour, are published separately (Vaz et al. 1997), where details on the photometry and on the reduction process are also given. Fig. 3 shows the y light curve and $b - y$ and $u - b$ colour index curves of the system in the instrumental system. The minima are similar and the secondary minimum is displaced slightly from phase 0.5. The stars are close to each other, but not in contact, causing the distortion effect seen in the light curve between the eclipses. The data from the five observing runs match each other very well, indicating stability both of the orbit and of the components. The small diaphragm precluded contamination of the measurements by all stars except the companion detected visually by van den Bos (1931) and present in the spectrograms. During the photometric analysis, the light of this third component has been subtracted from all light curves in order to yield coherent photometric elements for the system.

3.2. Ephemeris and period analysis

The first ephemeris of V906 Sco was determined by Leung & Schneider (1975). From all their data they found $P = 2^d785847 \pm 0^d000016$. We obtained from our observations, using the Kwee & van Woerden method (1956), the three times of primary minimum and one of secondary minimum shown in Table 6 where we also give as the first entry Leung & Schneider's one time of minimum. The errors in our determinations are calculated from the interagreement of the values of the four colours.

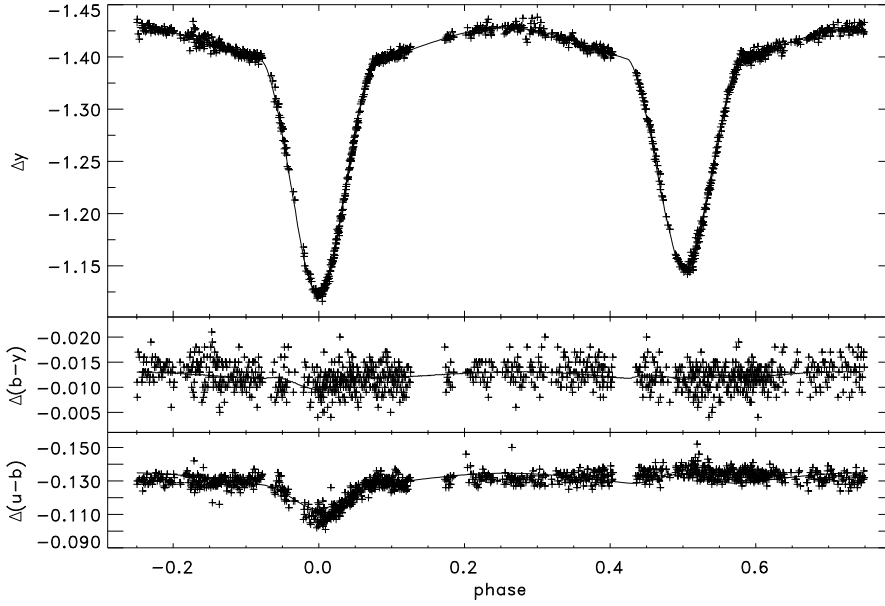


Fig. 3. y magnitude differences and $b - y$ and $u - b$ colour index differences between V906 Sco and HD 162631. The full line is the theoretical solution (number 12 in Table 8).

Table 6. Times of minimum of V906 Sco

HJD (-2 400 000)	type	O-C	E
39649.8163 ± 39	pri	$-0^d.0001$	-3125.0
47656.6312 ± 21	pri	$0^d.0024$	-251.0
48018.8006 ± 26	pri	$-0^d.0013$	-121.0
48355.9006 ± 18	pri	$0^d.0009$	0.0
48362.8747 ± 9	sec	$0^d.0083$	2.5

The period was determined with the Lafler & Kinman (1965) period-search method with all the observations yielding $P = 2^d.785957 \pm 0.000012$. With the 3 most recent times of primary minimum from Table 6 and a linear least-squares fit, we find

$$\text{MinI at : HJD} 2\,448\,355.8999 + 2^d.785934 E \quad (4)$$

$$\pm 15 \quad \pm 9$$

Introducing a larger number of cycles by including Leung & Schneider's (1975) primary minimum, recalculated by us with the Kwee & van Woerden (1956) method in order to have a homogeneous data set, we find:

$$\text{MinI at : HJD} 2\,448\,355.9015 + 2^d.785947 E \quad (5)$$

$$\pm 12 \quad \pm 8$$

which we adopt, giving the O-C of Table 6.

From the time of secondary minimum in Table 6 we notice that the secondary minimum does not occur at phase 0.5 but around 0.503. In order to verify if the orbit is really eccentric and not only shifted, we used the Kwee & van Woerden (1956) method to evaluate the position, in phase, of the primary and secondary minima and found: $\phi_{\text{pri}} = -0.00057 \pm 0.00027$ and $\phi_{\text{sec}} = 0.50266 \pm 0.00038$, which shows that only the secondary minimum is shifted and consequently the orbit is eccentric.

In order to check for apsidal motion we calculated the separation in phase of the minima of the UBV observations by Leung & Schneider (1975) using our ephemeris and obtained $\phi_{\text{sec}} - \phi_{\text{pri}} = 0.4964 \pm 0.0005$. Comparing it with the separation given by our observations, $\phi_{\text{sec}} - \phi_{\text{pri}} = 0.5031 \pm 0.0004$, apsidal motion is suggested. However, more times of minimum, especially for the secondary, are needed for it to be rigorously confirmed.

3.3. Photometric elements

The solutions were computed with the WD model (Wilson & Devinney 1971, Wilson 1979, 1993) in the modified version described by Vaz et al. (1995). Radial velocity curves and light curves were adjusted simultaneously, allowing us to check the consistency of the spectroscopic elements determined in Sect. 2. The system was found to be detached with both components in synchronous rotation. Tests with the gravity brightening exponent were done in an attempt to obtain a better fit for the u light curve.

3.3.1. Starting values and initial solutions

The mean temperature of the stars was estimated from the reddening-free index $[u - b]$. Using the Strömgren calibrations (1966) we have $[u - b] = 1.177$ which gives $T_{\text{mean}} = 10711$ K interpolating from Davis & Shobbrook (1977) tables. With the

Table 7. H_β observations of V906 Sco

HJD - 2 440 000	β	phase
7244.8859	2.799	0.209
7252.8531	2.805	0.069
7623.7686	2.800	0.206
7623.8589	2.801	0.239

Crawford (1978) calibrations we obtained $[u - b] = 1.186$ and $T_{\text{mean}} = 10667$ K. Four β observations were obtained and are listed in Table 7. Using the mean out-of-eclipse value of $\beta = 2.800$ and the Crawford (1978) calibrations we have $c_0 = 0.961$, which gives $T_{\text{mean}} = 10704$ K (Davis & Shobbrook, 1977). Following the calibration of Napiwotzki et al. (1993) and, again, using $[u - b]$ we find $T_{\text{mean}} = 10562$ K, about 150K below the values obtained with Davis & Shobbrook (1977) tables. Using the grids of Moon & Dworetzky (1985) and the relation between c_0 and β for the Kurucz (1979) atmospheres we find that our values match a temperature of 10700 K and a $\log g = 3.7$, values corresponding to spectral type B9 V according to Böhm-Vitense (1981). Anticipating that T_A would be only slightly higher than T_B and using the calibration of Napiwotzki et al. (1993) for T_{mean} , we adopted $T_A = 10700$ K while T_B was left free for adjusting.

The mass ratio, $q = M_B/M_A = 1.038 \pm 0.014$ (Sect. 2.2), was kept fixed at its spectroscopic value when just light curves were adjusted, but was left free in the final solutions where radial velocities were also adjusted.

The starting value of the third light was $L_3 = 0.1964$ (Sect. 2.3) for all colours. The gravity brightening exponents and the bolometric reflection albedos were initially fixed at 1.0 for both components (von Zeipel 1924), as is appropriate for atmospheres in radiative and hydrostatic equilibrium (Ruciński 1989).

The $\log g$ values used to calculate the limb darkening coefficients and to interpolate in the atmosphere tables of the model were redetermined at each new run. We used a linear limb darkening law, the coefficients being calculated by bi-linear interpolation from the tables published by Van Hamme (1993) and based on the model atmospheres of Kurucz (1979). The rotation rates (relative to synchronous rotation) of each star, important for the size calculations, were also redetermined at each run.

Due to the displacement of the secondary minimum from phase 0.5, the eccentricity, e , was not initially fixed. However, a strong correlation between e and ω , the angle of periastron passage, soon became evident, making impossible the convergence of any solution if both parameters were left free to vary. If just one of them was fixed, the other assumed values that did not reproduce the position of the secondary minimum, which depends on e , ω , i , the orbital inclination and P , the orbital period. As P is well determined (Sect. 3.2) and i converged rapidly in the initial solutions, we calculated a series of combinations for e and ω that would reproduce the position of the secondary minimum correctly. To estimate the range of acceptable values of e and ω we used $D_{\text{sec}}/D_{\text{pri}}$, the ratio of the duration of the minima,

ϕ_{pri} and ϕ_{sec} , their positions, the corresponding errors and the same procedure as used before in KW Hya (with the WINK model, Andersen & Vaz 1984, Vaz 1984, 1986). We determined $D_{\text{sec}}/D_{\text{pri}} = 1.00 \pm 0.03$, the error being slightly overestimated due to the lack of points in the beginning of the secondary minimum (see Fig. 3). In this process we used WINK applied to the individual colours in order to determine $e \cos \omega$ and $e \sin \omega$ and to improve our estimation of L_3 for each light curve. The difference in the minima central phases, $\phi_{\text{sec}} - \phi_{\text{pri}}$ (Sect. 3.2), yielded a relatively precise value for $e \cos \omega$ (0.0045 ± 0.0008), but the ratio $D_{\text{sec}}/D_{\text{pri}}$ affects $e \sin \omega$, which became poorly determined (0.0002 ± 0.0041). Then, by using both WINK and WD we could only establish that $-80^\circ \leq \omega \leq 80^\circ$ which corresponds to $0.004 \leq e \leq 0.028$. So we calculated solutions for the fixed values of $\omega = -75^\circ, -40^\circ, -20^\circ, 0^\circ, 40^\circ, 50^\circ, 75^\circ, 80^\circ$ and their corresponding eccentricity values.

Due to correlations between the parameters we first used the v curve to determine the geometric parameters, because L_3 for v is known approximately from the spectroscopy. By starting with only i as a free parameter, then adding the secondary temperature, T_B , and the gravitational potentials, and finally alternately adjusting L_3 and i we obtained a consistent set of geometric parameters. We then kept i and the gravitational potentials fixed for the other colours and determined L_3 for u , b , and y . In the final simultaneous solutions for all four colours (with or without the radial velocity curves) L_3 was kept fixed at those values. Note that the model input parameters $\mathcal{L}_{A,B}$ are 4π steradian luminosities (\mathcal{L}_B is automatically calculated by the code from the input temperatures and radii), while L_3 is in units of the apparent light from the eclipsing stars integrated in the observer's direction.

3.3.2. Final solutions with the WD model

The WD model was always used in mode 2 (detached system). The slight deformation, due to proximity effects, in the light curves between the eclipses was well reproduced, the final fits being very good and so confirming that the system is detached, with fill-out factors (F_{out} , Mochnacki 1984) for both components well below unity (Table 8).

In the final solutions the parameters to be determined by least-squares fitting were: the inclination, i , the temperature of the secondary, T_B , the gravitational potentials, Ω_A and Ω_B and the luminosity of the primary, \mathcal{L}_A , when only light curves were adjusted. When adjusting radial velocity curves for both components simultaneously with the $uvby$ light curves, we added to the above-mentioned list of adjustable parameters the mass ratio, q , the semi-major axis, a and the center of mass velocity, V_{CM} .

The solutions are presented in Table 8. For those with $\omega = \pm 75^\circ$ and $\omega = 80^\circ$ the residuals show systematic trends and we discard these solutions. The residuals for $\omega = 40^\circ$ are shown in Fig. 4, which refers to the adopted solution, Sol. 12. No systematic trends are seen in the $uvby$ plots, but the theoretical u curve did not reproduce accurately the observations for neither this nor any other value of ω . To solve this problem we

Table 8. WD solutions for V906 Sco. All the solutions were computed with the *wby* light curves and the solutions 1 to 7 and 12 (adopted) used the radial velocity curves, too. The σ values were calculated using only light curves.

param.	Sol. 1	Sol. 2	Sol. 3	Sol. 4	Sol. 5	Sol. 6	Sol. 7	Sol. 8	Sol. 9	Sol. 10	Sol. 11	Sol. 12 adopted
ω (fixed)	-75°	-40°	-20°	0°	40°	50°	75°	-20°	0°	40°	50°	40°
e (fixed)	0.0185	0.0064	0.0046	0.0048	0.0054	0.0075	0.0183	0.0046	0.0048	0.0054	0.0075	0.0054
a (R_\odot)	15.546 ± 10	15.557 ± 10	15.543 ± 10	15.566 ± 10	15.564 ± 10	15.567 ± 10	15.552 ± 11	– –	– –	– –	– –	15.634 ± 10
V_{CM} (km s^{-1})	-15.47 ± 7	-15.46 ± 7	-15.47 ± 7	-15.46 ± 7	-15.49 ± 7	-15.49 ± 7	-15.50 ± 8	– –	– –	– –	– –	-15.02 ± 7
q	1.0269 ± 13	1.0284 ± 13	1.0276 ± 13	1.0281 ± 13	1.0270 ± 13	1.0271 ± 14	1.0269 ± 14	1.038 fixed	1.038 fixed	1.038 fixed	1.038 fixed	1.0395 ± 13
i	$76^\circ 093$ ± 24	$76^\circ 176$ ± 27	$76^\circ 307$ ± 11	$76^\circ 124$ ± 12	$76^\circ 174$ ± 15	$76^\circ 200$ ± 29	$76^\circ 557$ ± 27	$76^\circ 201$ ± 7	$76^\circ 228$ ± 6	$76^\circ 106$ ± 5	$76^\circ 126$ ± 5	$76^\circ 154$ ± 14
T_{B} (K)	10231 ± 7	10327 ± 7	10361 ± 3	10354 ± 6	10384 ± 7	10391 ± 7	10442 ± 8	10425 ± 8	10398 ± 8	10383 ± 8	10351 ± 9	10397 ± 6
g_{A}	1.0 fixed	1.0 fixed	1.0 fixed	1.0 fixed	1.0 fixed	1.0 fixed	1.0 fixed	0.152 ± 74	0.401 ± 75	0.642 ± 71	0.981 ± 71	1.0 fixed
g_{B}	1.0 fixed	1.0 fixed	1.0 fixed	1.0 fixed	1.0 fixed	1.0 fixed	1.0 fixed	0.892 ± 21	0.863 ± 22	0.743 ± 21	0.671 ± 22	1.0 fixed
Ω_{A}	5.4466 ± 92	5.5549 ± 91	5.5978 ± 40	5.5219 ± 60	5.5216 ± 67	5.527 ± 10	5.4447 ± 92	5.5726 ± 22	5.5728 ± 24	5.5136 ± 19	5.5136 ± 22	5.5274 ± 63
Ω_{B}	4.6533 ± 62	4.6024 ± 57	4.6076 ± 19	4.6084 ± 45	4.6036 ± 44	4.6045 ± 57	4.6295 ± 61	4.5560 ± 19	4.5666 ± 19	4.5496 ± 17	4.5604 ± 18	4.6373 ± 52
$\mathcal{L}_{\text{A}}(u)$	5.991 ± 28	5.413 ± 22	5.261 ± 10	5.357 ± 19	5.350 ± 20	5.334 ± 24	5.613 ± 28	5.094 ± 12	5.155 ± 13	5.240 ± 13	5.304 ± 13	5.382 ± 19
$\mathcal{L}_{\text{A}}(v)$	5.288 ± 23	4.827 ± 18	4.832 ± 8	4.955 ± 16	4.802 ± 16	4.792 ± 20	5.074 ± 22	4.723 ± 8	4.788 ± 8	4.712 ± 7	4.753 ± 8	4.839 ± 15
$\mathcal{L}_{\text{A}}(b)$	5.185 ± 22	4.791 ± 18	4.880 ± 8	4.930 ± 16	4.766 ± 16	4.757 ± 20	4.994 ± 21	4.775 ± 7	4.766 ± 7	4.679 ± 7	4.717 ± 7	4.804 ± 15
$\mathcal{L}_{\text{A}}(y)$	5.088 ± 21	4.857 ± 18	4.829 ± 8	4.934 ± 16	4.841 ± 16	4.831 ± 20	4.913 ± 21	4.729 ± 7	4.772 ± 7	4.753 ± 7	4.790 ± 7	4.880 ± 15
$\mathcal{L}_{\text{B}}(u)$	7.6988	7.8323	7.8464	7.7010	7.7907	7.8044	7.9856	7.9434	7.9040	7.8384	7.7838	7.8816
$\mathcal{L}_{\text{B}}(v)$	7.4246	7.5109	7.7043	7.6215	7.4433	7.4539	7.5983	7.7877	7.7995	7.5119	7.4762	7.5231
$\mathcal{L}_{\text{B}}(b)$	7.3143	7.4606	7.7756	7.5830	7.3825	7.3922	7.4689	7.8529	7.7494	7.4493	7.4171	7.4616
$\mathcal{L}_{\text{B}}(y)$	7.2313	7.6084	7.7374	7.6325	7.5367	7.5463	7.3774	7.8130	7.7961	7.6057	7.5746	7.6173
$L_3(u)$	0.1993	0.2017	0.1996	0.1996	0.2049	0.2049	0.2564	0.1996	0.1996	0.2049	0.2049	0.2049
$L_3(v)$	0.2050	0.1998	0.2008	0.2008	0.2044	0.2044	0.2654	0.2008	0.2008	0.2044	0.2044	0.2044
$L_3(b)$	0.2017	0.1993	0.1977	0.1977	0.2011	0.2011	0.2622	0.1977	0.1977	0.2011	0.2011	0.2011
$L_3(y)$	0.2021	0.2042	0.1981	0.1981	0.2010	0.2010	0.2528	0.1981	0.1981	0.2010	0.2010	0.2011
$F_{\text{out,A}}$	0.7178	0.7005	0.6951	0.7028	0.7032	0.7039	0.7176	0.6981	0.7204	0.7036	0.7050	0.7056
$F_{\text{out,B}}$	0.8336	0.8342	0.8322	0.8323	0.8330	0.8336	0.8374	0.8412	0.8383	0.8407	0.8399	0.8310
r_{A} pole	0.2259	0.2201	0.2179	0.2215	0.2217	0.2216	0.2260	0.2191	0.2192	0.2219	0.2221	0.2218
r_{A} point	0.2344	0.2274	0.2249	0.2290	0.2292	0.2299	0.2342	0.2263	0.2263	0.2294	0.2297	0.2294
r_{A} side	0.2284	0.2225	0.2203	0.2239	0.2241	0.2240	0.2285	0.2215	0.2215	0.2243	0.2245	0.2242
r_{A} back	0.2325	0.2260	0.2236	0.2275	0.2277	0.2276	0.2325	0.2249	0.2250	0.2280	0.2282	0.2279
r_{B} pole	0.2784	0.2818	0.2813	0.2813	0.2814	0.2814	0.2803	0.2852	0.2844	0.2855	0.2846	0.2818
r_{B} point	0.2998	0.3035	0.3027	0.3027	0.3029	0.3031	0.3023	0.3078	0.3069	0.3083	0.3072	0.3032
r_{B} side	0.2844	0.2879	0.2873	0.2873	0.2874	0.2875	0.2863	0.2914	0.2906	0.2917	0.2908	0.2879
r_{B} back	0.2938	0.2974	0.2967	0.2967	0.2969	0.2970	0.2960	0.3013	0.3005	0.3017	0.3007	0.2973
σ (mag)	0.0042	0.0039	0.0039	0.0039	0.0039	0.0039	0.0040	0.0037	0.0037	0.0037	0.0037	0.0037

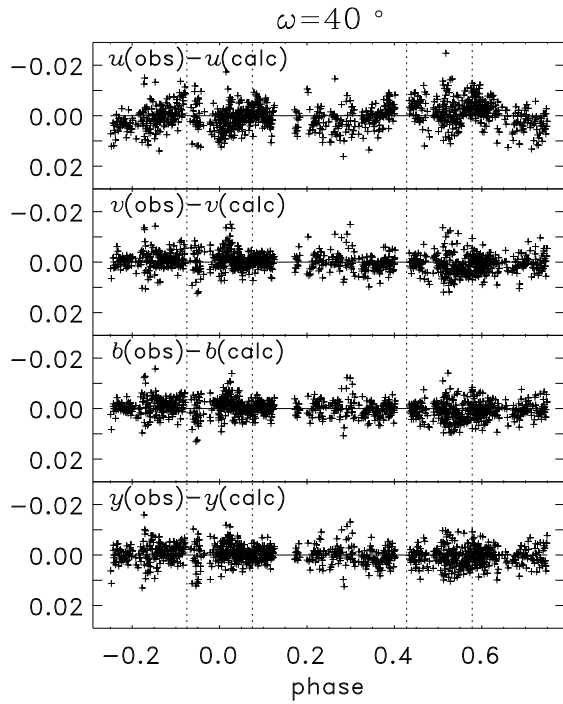


Fig. 4. Residuals of the *uvby* observations with fixed gravity brightening coefficients. The theoretical phases for the start and end of each eclipse are shown with dotted lines.

tried first to use a better description of the reflection effect in the model (Wilson 1990). Normally, approximate reflection is used, the star that illuminates the other being treated as a point source. We did some tests with detailed reflection, where the illuminating star is extended instead. Further, we used both single and multiple reflections. However, it was impossible to remove the systematic trends in residuals of the *u* curve with this procedure, indicating that their cause is not related to the model for the reflection effect.

Until now, the gravity brightening exponents, *g*, were fixed at 1.0, the theoretical value calculated by von Zeipel (1924) for radiative envelopes in hydrostatic equilibrium. By letting *g* vary we could obtain solutions that showed very little or no systematic trends in the residuals of any colour. However, the exponents determined are very different from the theoretical ones. In Table 8 we present the variation of g_A and g_B for some of the solutions.

The primary component is less massive than the secondary and therefore less evolved in the MS. We should, then, expect it to be better described by the theory than its companion. Assuming, then, that the gravity brightening exponent of the primary is close to 1, while the exponent of the secondary is not very far from it, a good solution is the one computed for $\omega = 50^\circ$ and variable values of *g* (solution 11 of Table 8). However, since both stars have atmospheres in radiative equilibrium, we decided to adopt the values determined with $\omega=40^\circ$ and $g=1$, although a better fit would be achieved if we could accept a solution with $g < 1$ for the components of V906 Sco.

Table 9. Mean elements for V906 Sco

<i>i</i>	$76^\circ 154 \pm 0^\circ 063$	$L_B/L_A(\text{visual})$	1.59 ± 0.27
<i>e</i>	$0.0054^{+0.0020}_{-0.0010}$	ω	$40^\circ^{+10}_{-60}$
T_B/T_A	0.9717 ± 0.0022	$(T_A = 10\,700\text{ K assumed})$	
Ω_A	5.527 ± 0.031	Ω_B	4.637 ± 0.031
$r_{\text{vol},A}$	0.2248 ± 0.0025	$r_{\text{vol},B}$	0.2892 ± 0.0022

Table 10. Individual *uvby* standard indices for the components of V906 Sco (not corrected for reddening)

index	A	B	C
\bar{V}	7.18	6.70	7.90
<i>b - y</i>	0.029	0.034	0.032
m_1	0.107	0.100	0.086
c_1	0.930	0.996	0.984

By starting from the adopted values above, we applied WD again to the individual light curves and the results were in agreement with each other in all 4 colours and consistent with solution 12 (Table 8).

The final mean elements for V906 Sco are presented in Table 9. They were calculated with solution 12 in Table 8, in which we adjusted the light curves together with the radial velocity curves, but agree within their errors with all the possible solutions (sols. 3, 4, 5, and 6 for *g* fixed and sols. 8, 9, 10, 11 for *g* variable). Solution 12 differs from sol. 5 in Table 8 by having a more correct value for the mass ratio as well as having WD corrections due to the reflection effect included in the radial velocities. The rms of the O-C in the best solutions of Table 8 is even smaller than the intrinsic observational errors in each colour (Sect. 3.1). It must be noted that while the parameter values in Table 9 were taken from solution 12 the errors quoted are larger than those found for that solution. They were calculated from the spread in parameter values found when comparing all nine acceptable solutions from Table 8 (no matter if *g* was fixed or adjusted, and with $-20^\circ \leq \omega \leq 50^\circ$), and taking into account the spread in solutions for individual colours. By choosing these mean errors for our results we have fully accounted for the uncertainties in ω , *e* and in the best treatment for the gravity brightening effect.

By using the luminosity ratios from our final solution (12 in Table 8), together with data from Table 1, we can also calculate individual Strömgren indices and estimate individual temperatures for the three stars in the same manner as was done in Sect. 3.3.1 for the combined system. We obtain the indices of Table 10 and $T_A = 10815\text{ K}$ (Davis & Shobbrook 1977), $T_A = 10722\text{ K}$ (Napiwotzki et al. 1993), in very good agreement with our adopted $T_A = 10700\text{ K}$. The same values for T_B are 10543 K and 10428 K, respectively, and the temperature ratio agrees with that of Table 9. For the third star, temperatures are 10745 K and 10647 K, respectively, which confirms that it has almost the same spectral type as the eclipsing pair.

Table 11. Astrophysical data for V906 Sco

	A (Primary)	B (secondary)
Absolute dimensions:		
mass (M_{\odot})	3.253 ± 0.069	3.378 ± 0.071
radius (R_{\odot})	3.515 ± 0.039	4.521 ± 0.035
$\log g$ (cgs)	3.858 ± 0.013	3.656 ± 0.012
V_{synchr} (km s^{-1})	63.1 ± 0.7	82.8 ± 0.7
$V_{\text{rot}}/V_{\text{synchr}}$	0.98 ± 0.13	0.97 ± 0.06
Photometric data:		
T_{eff} (K)	10700 ± 500	10400 ± 500
$\log L/L_{\odot}$	2.162 ± 0.082	2.330 ± 0.084
M_{bol}	-0.71 ± 0.20	-1.14 ± 0.21
M_V	-0.31 ± 0.20	-0.82 ± 0.21
Distance (pc)	283 ± 20	

4. Discussion

4.1. Interstellar absorption and bolometric corrections

The effects of reddening and absorption were estimated using the Crawford (1978) calibrations. With the standard values for star A from Table 10 (the least evolved of the eclipsing components) and Crawford's relations we obtained $c_0=0.919$, $E(b-y)=0.059$ and $A_V=0.242\pm 0.032$. As V906 Sco is a member of the open cluster M 7 (see Sect. 4.2), we could also use the interstellar absorption values published for the cluster. Snowden (1976) calculated $A_V=0.25\pm 0.08$, while Nissen (1988), using $wby\beta$ measurements of F stars, found $A_V=0.160\pm 0.025$. Although these values differ from each other, they are in agreement within the errors. Due to that, we could have adopted a mean value between them, $A_V=0.205\pm 0.06$, which also agrees with our determination. However, we suspect some of the stars used by Nissen (1988) to be multiple (see Sect. 4.3), which would affect his interstellar absorption value, and as Snowden's (1976) A_V value has a large uncertainty, we finally decided to adopt our determination, $A_V=0.242\pm 0.032$, as the cluster interstellar absorption.

The effective temperatures of the eclipsing stars (Table 11) yield, together with Popper's (1980) tables, the bolometric corrections $BC_{\text{pri}}=-0.40$ and $BC_{\text{sec}}=-0.32$.

4.2. Absolute dimensions

The results of the previous section together with the spectroscopic and photometric parameters from Tables 4 and 8 were used to compute the absolute physical parameters of V906 Sco presented in Table 11. $M_{\text{bol},\odot}$ was taken to be 4.69 (Lang 1974). The accuracy of 1-2% in the absolute dimensions makes V906 Sco a reliable system for tests of stellar structure models. Four other binary systems with components of mass similar to V906 Sco, χ^2 Hya (Andersen 1975; Clausen & Nordström 1978), IQ Per (Lacy & Frueh 1985), V451 Oph (Clausen et al. 1986) and PV Cas (Popper 1987), have absolute dimensions determined with the same percentage errors. The last three systems have slightly eccentric orbits showing apsidal motion as

V906 Sco does, but are less evolved than the latter. The primary component of χ^2 Hya, although more massive than both components of V906 Sco, has an intermediate $\log g$ value and is closest to V906 Sco's components in a $\log g$ vs. $\log T_{\text{eff}}$ diagram. Fortunately, both components of V906 Sco are evolved main sequence stars, the secondary being near the TAMS and lying in a region of low data density.

V906 Sco was considered a member of M 7 in all cluster analyses in which it was included (Koelbloed 1959; Abt et al. 1975; Snowden 1976; Eggen 1981). Some recent distance determinations for M 7 are $d = (251 \pm 45)$ pc (Snowden 1976), (249 ± 41) pc (Eggen 1981), and (252 ± 23) pc (Nissen 1988). The distance we obtain for the system, $d = (283 \pm 20)$ pc, is somewhat larger than the cluster distance although in agreement within the formal errors. The uncertainty in A_V cannot explain the discrepancy. However, if binaries have polluted the cluster samples an error in distance modulus of 0.3 can easily arise. The radial velocity we obtain for the system, (-15.0 ± 0.8) km s^{-1} , matches excellently the cluster radial velocity of (-15.3 ± 0.5) km s^{-1} as determined by Giesecking (1985).

4.3. Evolutionary models

The values of $\log g$ and $\log T_{\text{eff}}$ determined in the previous section are plotted in Fig. 5 together with evolutionary tracks and an isochrone for solar metallicity calculated with recent overshooting models (Claret 1995).

Models with lower metallicity ($Z=0.01$) did not fit well the components of V906 Sco. There is a general tendency that *young* B stars have a metal abundance *lower* than solar (Andersen et al. 1993; Nordström & Johansen 1994 and references therein). On the other hand, other more evolved late B - early A systems (χ^2 Hya, Clausen & Nordström 1978; V541 Oph, Clausen et al. 1986; V1647 Sgr, Andersen & Giménez 1985; GZ CMa, Popper et al. 1985; V1031 Ori, Andersen et al. 1990a; KW Hya, Andersen & Vaz 1984; V539 Ara, Clausen 1996) are well represented (V539 Ara is in fact *better* represented) by models with solar composition. This is contrary to what we expect for galactic chemical evolution, which predicts that the interstellar environment should on average increase its metallicity due to dying stars. All these stars are inside a volume of radius ≈ 2000 pc from the Sun, so that a galactic metallicity gradient is not the answer. Whether this puzzling finding is due to remaining inaccuracies in the models or has an entirely different cause remains to be seen.

In Fig. 5 we also show the $3.2 M_{\odot}$ track determined with a standard model (Claret & Giménez 1989). According to the standard model, the secondary component would lie in the unlikely region of the Hertzsprung gap in the HR diagram. The evolutionary model with convective overshooting places both evolved components inside the main sequence, a much more acceptable situation.

Fig. 5 shows one track for the secondary component and three tracks for the primary star, corresponding to our final mass value and the 1σ interval. The agreement between the

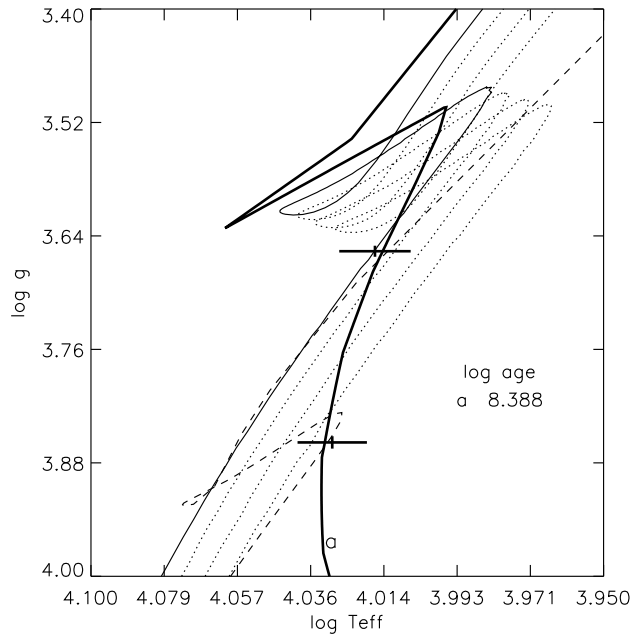


Fig. 5. The thin solid line corresponds to the evolutionary track calculated for the secondary component, the dotted lines to tracks calculated for the primary, and the thick solid line is the isochrone for the system. The tracks and isochrones are from Claret’s models (1995) for the relevant masses and $\log(\text{age})$ and, for the primary component mass, for its 1σ confidence interval. The dashed line is the $3.2 M_{\odot}$ standard model. The chemical composition of all models is $X = 0.70$, $Z = 0.02$. The positions of the eclipsing stars and their 1σ uncertainties are also shown.

Table 12. Age, circularization and synchronization of V906 Sco, using the models by Claret (1995).

$\log \text{age A}$	8.414 ± 0.020
$\log \text{age B}$	8.361 ± 0.019
$\log \text{age (system)}$	8.388 ± 0.027
Circularization:	
T_{cri}	$8.14^{+0.22}_{-0.11}$
Synchronization:	
$T_{\text{cri A}}$	$6.55^{+0.12}_{-0.08}$
$T_{\text{cri B}}$	$6.55^{+0.12}_{-0.10}$

secondary and the model is excellent and, although the results for the primary do not match the model so well, they do agree within the errors. The common isochrone fits both components and determines the system’s age (Table 12). As V906 Sco is a member of the open cluster M 7, that age should also correspond to the age of the cluster. Meynet et al. (1993) have determined the age of M 7 by fitting an isochrone to the cluster colour-magnitude diagram, using the models by Schaller et al. (1992) with moderate overshooting and solar metallicity. They obtain $\log \text{age} = 8.350 \pm 0.020$, which agrees with our value (Table 12), confirming through completely different and independent methods the age of M 7.

By taking $B-V$ and $b-y$ data for M 7 from Meynet et al. (1993), Nissen (1988), Snowden (1976), and this work, we

Table 13. Transformation coefficients for Eq. 6, obtained from 46 stars in the M 7 region.

a_0	a_1	a_2
-0.0491	1.880	-0.361
± 90	± 62	± 52

derived the transformation equation (indices not corrected for reddening)

$$(B - V) = \sum_{i=0}^2 a_i (b - y)^i \quad (6)$$

with coefficients a_i given in Table 13.

This equation was used to transform Nissen’s (1988) $(b - y)$ data for M 7 as well as our $(b - y)$ for the components of V906 Sco (Table 10) to $B-V$. With the relation $E(B - V) = E(b - y)/0.74$ (Crawford 1978) and $E(b - y)$ as adopted in Sect. 4.1 we then obtained $(B - V)_0$. Figure 6 shows these data and also those from Meynet et al. (1993) and the isochrone from Claret (1995, Fig. 5) calculated for our value for $\log \text{age}$. $(B - V)_0$ for the Meynet et al. data were obtained from $E(B - V) = A_V/3.1$ and $A_V = 0.242$, determined in Sect. 4.1. We transformed the V apparent magnitudes to absolute ones with the same A_V and a distance modulus of 7.15, intermediate between that obtained from our data (Table 11) and that determined for M 7. The full circle corresponds to the triple system V906 Sco as measured by Meynet et al. (1993) and is connected to a filled square, our value for the system. The open circles and squares connected by lines are measurements of the comparison stars C_1 and C_2 from Meynet et al. (1993) and Table 1, respectively, and the large crosses show the positions of the individual components of V906 Sco. We note that the isochrone fits the cluster data very well, which also means that there is excellent agreement between the cluster age and our age determination for V906 Sco.

Three stars observed by both Meynet et al. (1993) and Nissen (1988) are also connected by lines. One of them was suspected by Nissen to be multiple and is marked in the figure overplotted with a small cross. However, Fig. 6 shows clearly that this is not the only star used by Nissen that is likely to be multiple (note in Fig. 6 how far the individual components of V906 Sco lie from the combined system). In fact, there is a reasonable probability that the F stars used by Nissen are wide pairs with long periods and different masses, as the mean brightness difference between the stars and the isochrone is less than $0^m.75$, the expected magnitude difference between a single star and a system composed of two equal stars. As Nissen used a limited spectral-type range in his study, he had no means to suspect that many of his stars may be multiple, despite Giesekeing’s (1985) conclusion that the binary frequency in M 7 is near 100%. An immediate consequence of this is that the distance derived by Nissen (1988) is smaller (but still the results agree within their errors) than the one determined by us. Likewise, his value for

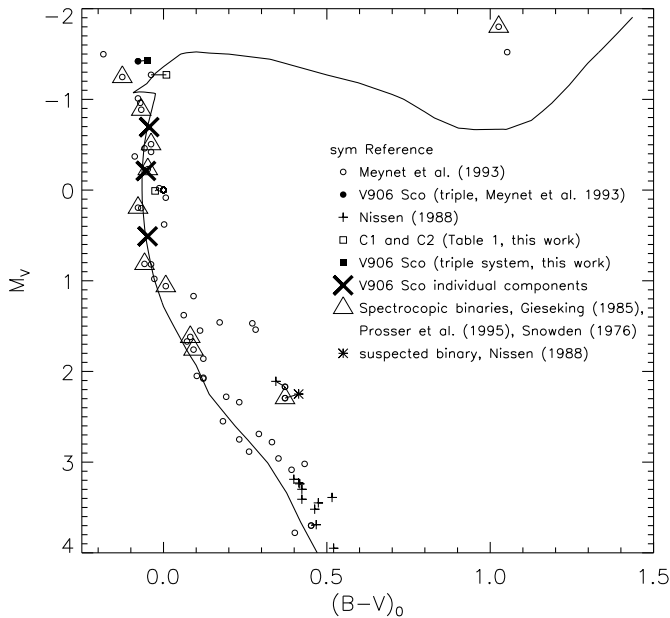


Fig. 6. Measurements of M 7 members. The solid line corresponds to the isochrone from Claret (1995) at $\log \text{age} = 8.388$ (see also Fig. 5). The *uvby* observations were transformed as described in the text. The data points for the triple system V906 Sco are marked by filled symbols, while our values for the individual components are marked by large crosses: from top to bottom components B, A, and C. When a star used by Meynet et al. (1993, \circ , \bullet) was also observed by us (\square , \blacksquare) or by Nissen (1988, $+$), its points are connected by lines. The star overplotted with a \times was marked by Nissen as a suspected multiple star. The spectroscopic binaries listed by Giesekeing (1985), Snowden (1976) and by Prosser et al. (1995) are overplotted with a \triangle . In fact, several of Nissen’s stars are likely to be multiple.

the interstellar absorption will become too small (see Sect. 4.1).

There is an apparent contradiction between the effective temperatures (Sect. 3.3.2) and masses for the components, as we found that the most massive (component B) is the coldest, while the least massive (component C, as inferred from its evolutionary stage in Fig. 6) has an intermediate temperature. The shape of the isochrone (Figs. 5 and 6) and the evolutionary stage of the three components are the reason for this effect and our picture for all three components of the system is fully consistent. Our solution for the third component’s light contribution is quite consistent with it being a normal star with a mass $\approx 3 M_{\odot}$ and thus the least evolved of the system.

4.4. Orbit circularization

Cunha (1995) kindly calculated the critical times of synchronization and circularization of the system (Tab. 12), using the models by Claret (1995) for solar metallicity and the procedure described in Claret et al. (1995). The critical times for synchronization are much smaller than the age of the system, agreeing with our result (Table 12) that the rotation of the stars is synchronized with the orbit.

However, according to the models, the orbit should already be circular and this disagrees with the photometric observations. In Section 3.3.2 we determined the orbital eccentricity ($e = 0.0054^{+0.0020}_{-0.0010}$, from Table 9), and even though it is very small, it is definitely not zero. The calculations in Table 12 were performed assuming that V906 Sco is a double system, and therefore neglecting the possible influence of the third star on the orbit of the binary pair. According to Mazeh (1990), a third component can slightly modulate the eccentricity of a binary pair, making it possible to find eccentric orbits after a time greater than the circularization time predicted by theoretical models. Mazeh & Shaham (1979) found that the eccentricity modulation is periodic, with a period:

$$P_{\text{mod}} \approx P_3 \frac{P_3 (M_A + M_B + M_3)}{M_3} \quad (7)$$

where P_3 is the orbital period of the third star and M_3 its mass. For V906 Sco, $P \approx 2^{\text{d}}78$, and the third component has a spectral type close to B9 (see Sect. 2.2), so that M_3 is of the order of the masses of the two other components. We can give a rough estimate only of P_3 . In 1929 the system was observed as a visual binary with an angular separation of $0''.3$ and in 1957 the angular separation had decreased to $0''.1$ (Index Catalogue of Visual Double Stars), while thirty years later we did not resolve the system as a visual binary. This indicates that P_3 is at least of the order of a hundred years, leading to a P_{mod} of the order of a million years, so that the system could be observed with a constant eccentricity for more than a hundred years. Mazeh & Shaham found modulation amplitudes of typically a few hundredths which supports the view that the eccentricity of 0.0054 found by us is caused by this effect.

4.5. Apical motion

From the orbital eccentricity, masses, and radii given above it is possible to estimate limits for the apical motion period, by following Martynov (1973). Assuming that the stars are synchronized with the orbital motion and that the values of the mean density concentration coefficients for real stars are between those of polytropic index $n = 3$ and $n = 4$ (Martynov 1973), we find that the lower and upper limits for the apical motion period U (due only to tidal and rotational deformation) are $U_{\text{min}} = 1500 P$ (for $n = 3$) and $U_{\text{max}} = 16000 P$ ($n = 4$), which correspond approximately to 12 yrs and 125 yrs, respectively.

The influence of the third companion may also be estimated. The mass fraction, relative to the total mass of the eclipsing system, of the third companion is $\lesssim 0.5$ (similar spectral types, see Fig. 6) and the wide orbit period P_3 has been estimated in the previous section. Assuming coplanar orbits (wide and close) and that the angular velocity vectors are parallel (Martynov 1973), we estimate a lower limit for the advance of the line of apsides (caused only by the presence of the third body in the system) of $U_{3\text{rd}} = 16000 P$, or ~ 1200 yrs. The contribution to the apical rotation due to the third component is then much smaller than the tidal and rotational deformation terms.

Using a different approach, we have taken the values for the density concentration coefficients, $\log k_2$, $\log k_3$, and $\log k_4$ for each component, from direct integration in the evolutionary models (Claret 1995). With these values and again following Martynov (1973) we find $U_{\text{model}} = 4900 P$. Considering that the relative error in our determination of the eccentricity is large (0.5), we predict that $U_{\text{model}} = 37 \pm 18$ yrs.

Then, the apsidal motion detected in Sect. 3.2 is very plausible and it would be highly desirable (and not very difficult) to measure it, considering the reasonably short estimated period of ~ 40 yrs. This information, together with the accurate absolute dimensions of V906 Sco, may provide more critical tests for evolutionary models especially in the final stages of the main sequence.

5. Conclusions

We have obtained new radial velocity curves and light curves for V906 Sco. The precise absolute dimensions derived from these data (errors of $\approx 2\%$ in the masses and $\approx 1\%$ in the radii) show that the eclipsing system has components approaching the TAMS, according to evolutionary models with convective core overshooting, and that standard models (without overshooting) cannot represent the system. The masses and evolutionary status of the components of V906 Sco place them in the $\log g$ vs. $\log T_{\text{eff}}$ and in the H-R diagrams at positions that can be very well fitted by a single isochrone.

V906 Sco is yet another system that confirms the need, in this mass range, for models with convective core overshooting, like LZ Cen (Vaz et al. 1995) and other systems summarized by Andersen (1991) and Andersen et al. (1990b). Like other late B - early A systems in this mass and age range, but unlike young B stars, only models with solar composition gave good fits. Thanks to the system being in a very evolved main sequence phase and having at the same time an apsidal motion with, probably, a rather short period, V906 Sco may prove extremely useful for further tests of evolutionary models.

The triple system V906 Sco is a member of M 7 and a classical example of a hierarchical binary, combining a visual pair with an eclipsing system. Our distance determination for V906 Sco agrees within the formal errors with the cluster distance, and our values for its radial velocity and age are in excellent agreement with the cluster values. The intrinsic indices calculated from our solution are completely self-consistent for the three components, indicating that the visual component is less evolved than the eclipsing ones, but of the same age. During the time interval covered by our observations (from 1987 to 1995) the components of the visual pair (V906 Sco and its companion) were so close that it was impossible to resolve them at the telescope. As the system has been detected as a visual binary before (van den Bos 1931), it would be desirable to follow the visual orbit. This may provide important insight into the dynamics of multiple systems, particularly concerning the spin-orbit coupling.

Acknowledgements. Observing time on the Strömgren Automatic Telescope (SAT) at ESO was made available through the Danish Board for

Astronomical Research; on the 1.6 m at LNA, Brasópolis, Brazil, the assignment of observing time was done by the LNA Scientific Programme Commission. This work has been supported by the following Brazilian institutions: FAPEMIG, CNPq, FINEP, CAPES, and in Denmark by The Danish Natural Science Research Council. Fruitful discussions with Dr. J.V. Clausen are gratefully acknowledged. This research has made use of the Simbad data base, operated by the CDS, Strasbourg, France.

References

- Abt H.A., Levy S.G., Baylor L.A., Hayward R.R., Jewsbury C.P., Snell C.M., 1970, *ApJ* 159, 919
 Andersen J., 1975, *A&A* 44, 445
 Andersen J., 1991, *A&ARS* 3, 91
 Andersen J., Giménez A., 1985, *A&A* 145, 206
 Andersen J., Vaz L.P.R., 1984, *A&A* 130, 102 (ERRATUM, 1987, *A&A* 175, 355)
 Andersen J., Clausen J.V., Nordström B., 1984, *A&A* 134, 147
 Andersen J., Clausen J.V., Nordström B., 1990a, *A&A* 228, 365
 Andersen J., Nordström B., Clausen J.V., 1990b, *ApJ* 363, L33
 Andersen J., Clausen J.V., Giménez A., 1993, *A&A* 277, 439
 Böhm-Vitense E., 1981, *ARA&A* 19, 295
 Claret A., 1995, *A&AS* 109, 441
 Claret A., Giménez A., 1989, *A&AS* 81, 1
 Claret A., Giménez A., Cunha N.C.S., 1995, *A&A* 299, 724
 Clausen J.V., 1996, *A&A* 308, 151
 Clausen J.V., Nordström B., 1978, *A&A* 67, 15
 Clausen J.V., Giménez A., Scarfe C., 1986, *A&A* 167, 287
 Crawford, D. L., 1978, *AJ* 83, 48
 Cunha N.C.S., 1995, Private Communication
 Davis J., Shobbrook R.R., 1977, *MNRAS* 178, 651
 Eggen O.J., 1981, *ApJ* 246, 817
 Etzel P.B., 1985, "SBOP – Spectroscopic Binary Orbit Program", Program's Manual
 Feinstein A., 1961, *PASP* 73, 452
 Giesekeing F., 1985, *A&AS* 61, 75
 Hill G., Khalessch B., 1991, *A&A* 245, 517
 Horne K., 1986, *PASP* 98, 609
 Kitamura M., Nakamura Y., 1986, *Ann. Tokyo Astron. Obs*, 2nd Ser. 21, 229
 Koelbloed D., 1959, *Bull. Astr. Inst. Neth.* 14, 265
 Kurucz R.L., 1979, *ApJS* 40, 1
 Kwee K.K., van Woerden H., 1956, *Bull. Astron. Inst. Neth.* 12, 327
 Lacy C.H., Evans D.S., 1979, *IBVS* 1704, 1
 Lacy C.H., Frueh M.L., 1985, *ApJ* 295, 569
 Lang K.R., 1974, in: *Astrophysical Formulae, a compendium for the Physicist and Astrophysicist*, Springer-Verlag, p. 565
 Laffer J., Kinman T.D., 1965, *ApJS* 11, 216
 Lehmann-Filhés R. 1894, *AN* 136, 17
 Leung, K.-C., Schneider, D.P., 1975, *ApJ* 201, 792
 Lucy L.B., 1967, *Zeitschr. für Astrophys.* 65, 89
 Martynov D.Ya., 1973, in: *Eclipsing Variable Stars*, ed. V.P. Tsesevich, IPST Astrophysics Library, Jerusalem, p. 270
 Mazeh T., 1990, *AJ* 99, 675
 Mazeh T., Shaham J., 1979, *A&A* 77, 145
 Meynet G., Mermilliod J.-C., Maeder A., 1993, *A&AS* 98, 477
 Mochnacki S.W., 1984, *ApJS* 55, 551
 Moon T.T., Dworetzky M.M., 1985, *MNRAS* 217, 305
 Napiwotzki R., Schönberner D., Wenske V., 1993, *A&A* 268, 653
 Nielsen R.F., Nørregaard P., Olsen E.H., 1987, *ESO Messenger* 50, 45

- Nissen P.E., 1988, *A&A* 199, 146
Nordström B., Johansen K.T., 1994, *A&A* 282, 787
Popper D.M., 1980, *ARA&A* 18, 115
Popper D.M., 1987, *AJ* 93, 672
Popper D.M., Andersen J., Clausen J.V., Nordström B., 1985, *AJ* 90, 1324
Prosser C.F., Stauffer J.R., Caillault J.-P., Balachandran S., Stern R.A., Randich S., 1995, *AJ* 110, 1229
Ruciński S.M., 1989, *Comments Astrophys.* 14, 79
Schaller G., Schaerer D., Meynet G., Maeder A., 1992, *A&AS* 96, 269
Slettebak A., Collins II G.W., Boyce P.B., White N.M. Parkinson T.D., 1975, *ApJS* 29, 137
Snowden M.S., 1976, *PASP* 88, 174
Sterne T.E., 1941, *Harvard Coll. Astron. Obs. Reprint* 222
Strömgren, B.: 1966, *ARA&A* 4, 433
van den Bos W.H., 1931, *Union Obs. Circ.* 85
Van Hamme W., 1993, *AJ* 106, 2096
Vaz L.P.R., 1984, Ph. D. Thesis, Copenhagen University Observatory (unpublished)
Vaz L.P.R., 1986, *Rev. Mex. Astron. Astrofis.* 12, 177
Vaz L.P.R., Andersen J., Rabello Soares M.C.A., 1995, *A&A* 301, 693
Vaz L.P.R., Andersen J., Clausen J.V., Helt B.E., García J.M., Giménez A., Alencar S.H.P., 1997, submitted to *A&AS*
Vieira E.F., 1991, M. Sci. Dissertation, Physics Dept., Federal University of Minas Gerais, Brazil
Vieira E.F., 1993, Trabajo de Investigación del Tercer Ciclo, Astrophysics Dept., Universidad Complutense de Madrid, Spain
von Zeipel H., 1924, *MNRAS* 84, 665
Wilson R.E., 1979, *ApJ* 234, 1054
Wilson R.E., 1990, *ApJ* 356, 613
Wilson R.E., 1993, in *New Frontiers in Binary Star Research*, eds. K.C. Leung and I.-S. Nha, *ASP Conf. Series* 38, 91
Wilson R.E., Devinney E.J., 1971, *ApJ* 166, 605
Wolfe Jr. R.H., Horak H.G., Storer N.W., 1967, in *Modern Astrophysics*, ed. M. Hack, Gauthiers–Villars, Paris, and Gordon and Breach, New York, p. 251